

The Pennsylvania State University  
College of Earth and Mineral Sciences  
Department of Geosciences

**Implications of Seafloor Expulsion Features of the Auger Basin, Deep  
Water Gulf of Mexico**

A Senior Thesis in Geosciences

by

Joshua F. Dixon

May, 2007

We approve this thesis:

---

\_\_\_\_\_  
Peter B. Flemings, Professor of Geosciences  
Date  
Thesis Advisor

---

\_\_\_\_\_  
David M. Bice, Professor of Geosciences  
Date  
Associate Head of the Undergraduate Program

# **IMPLICATIONS OF SEAFLOOR EXPULSION FEATURES OF THE AUGER BASIN, DEEP WATER GULF OF MEXICO.**

**Joshua Francis Dixon**

*Department of Geosciences, Pennsylvania State University, University Park,  
Pennsylvania 16802.*

## **ABSTRACT**

**Pore pressures in a hydrocarbon-producing sand body equal the overburden stress in the overlying seal in lease Block GB424 Auger Basin, deepwater Gulf of Mexico. I interpret that high pore pressure within the sand horizon is causing fractures within the overlying seal to dilate, which allows fluid venting from the sand crest. Leaking at the sand crest limits the reservoir pore pressure to that of the overburden stress at the crest. Leak points lie beneath mud volcanoes with localized biological communities, authigenic carbonate mineralization and gas hydrates. Pressure can be calculated at any point in a hydraulically connected basin if we know the least principle stress at the basin leak point.**

## INTRODUCTION

Previous work in the Auger Basin (Figure 1) and adjacent basins of the Gulf of Mexico continental slope has characterized the sedimentological and chemical processes occurring at active fluid expulsion features (Aharon, 2003, Anderson and Bryant, 1990, Brooks, et al., 1986, Lee, 1995, MacDonald, et al., 1990, 1994 and 2000, Roberts, et al., 1990, Sager, et al., 1999, Seldon and Flemings, 2005). Gas and fluid expulsion from such features are of broad interest as they relate to localized pollution, gas hydrate accumulation and petroleum exploration hazards (Seldon and Flemings, 2005).

Fluid expulsion from underlying aquifers occurs when pore pressures are elevated to the point where they exceed the least principle stress (Seldon and Flemings, 2005). Overpressure occurs when the rate of burial exceeding the ability of fluids to escape forcing the pore fluids to become a load-bearing component (Harrison and Summa, 1991, Seldon and Flemings, 2005). This overpressure of aquifers in sand bodies is intensified in dipping sand bodies encased in shales. In this case, pore pressure in shales follows a steeper (often lithostatic) pressure gradient, whereas pore pressure in sands follows the hydrostatic gradient (Flemings, et al., 2002). This results in a pressure field where the pore fluid pressure at the sand crest can converge on the least principle stress (Flemings, et al., 2002).

When the least principle stress at a sand crest exceeds the confining overburden stress, a leak point is produced. The sand crest is the point at which the sand reaches its minimum depth, and in the Auger Basin setting,

this is also where the sand body terminates (see Figure 2). A leak point is characterized by the creation or reactivation of pre-existing fractures in the overlying seal, which permit the flow of fluid as long as the aquifer remains in the state of pore pressure exceeding overburden stress (Hubbert and Willis, 1972, Cathles and Smith, 1983). Once pressures within the sand aquifer falls back below the overburden stress, the fractures are resealed and fluid expulsion terminates. This leaking and re-sealing process produces a maximum limit on pore pressure within an aquifer limited to the overburden stress at the sand crest leak point.

We mapped seafloor and four underlying sand horizons. Based on the mapped sand geometry, we then calculated the pore pressure throughout each sand body. We then showed that in one horizon the pore pressure equals the overburden stress, and we interpret the overlying mud volcanoes as being sourced from this sand.

## **GEOLOGY OF THE AUGER MINI-BASIN**

The Auger basin lies 350km southwest of New Orleans in the Garden Banks (GB) region of the central Gulf of Mexico slope (Figure 1, inset). Salt-cored ridges form a continuous bathymetric high bounding the basin on the west, south, east and parts of the north side of the basin. These salt bodies were intruded late in the history of the basin and post-date deposition of the reservoir of the Auger Field (Billinski, et al., 1995). The northern limit of the Auger Basin is defined by both the north-plunging Auger salt ridge, and the north Auger fault (Figure 10), which separated the Auger from the Andros

basin to the north in the Pliocene (Booth, et al., 2003) (Figure 1). Salt withdrawal in the Auger region has produced the convex down geometry of the basin fill, with all 4 sand horizons explored in this study onlapping onto these basin flanking ridges (Figure 5, 10).

Evidence for seepage of oil was recognized by MacDonald, et al. (2000) who identified periodic generation of oil slicks at the sea surface above the western basin flanking ridge of the Auger Basin using synthetic aperture radar (SAR). These surface oil slicks nucleated 6 times, covering areas of up to 1000 hectares during the 10 month study period. Several seafloor expulsion features have been identified on the western basin flanking ridge (MacDonald et al. 2000, Aharon, 2003, Sager, et al. 1999) by means of interpretation of their seismic reflection characteristics and direct imaging/sampling.

### **Reservoir Sand Characterization**

The progradation of continent-derived sediments throughout the Cenozoic produce a distal-to-proximal evolution with time in the stratigraphic column of the Gulf of Mexico. In the Auger basin this is expressed by the change from deposition of lower sheeted turbidite lobe sand geometries to channelized geometries. This has been interpreted in other areas as a response of the evolution from a rapidly subsiding basin with constant generation of accommodation space (distal sheeted deposits) to a slowly subsiding basin with limited accommodation space (channelized proximal deposits) through the progradation and seaward shift of proximal facies (Mutti

and Normark, 1987, Mutti and Ricci Lucchi, 1972, Normark, 1978, Walker, 1978). This change in depositional trend over time produced much more permeable and laterally continuous sands in the lower sheeted geometric section, with lateral flow quality decreasing in shallower, younger sands.

The pay section in Shell's Auger field below the Tension Leg Platform (TLP) (Figure 1) consists of stacked sands containing 5 major hydrocarbon pays, with the basal 3 (Pink, Red, Green) being in the lobe/sheet sands and the upper 2 (Blue, Yellow) being in the channelized sands deposited after a transition in depositional style coincident with the Pliocene-Pleistocene boundary (McGee, et al., 1994).

### **The 'PINK' Sand**

The lower Pliocene (McGee, et al. 1994) Pink sand has a gross thickness >200' consisting of coarsening up packages of turbidite lobe-derived sheet sands (McGee, et al., 1994). The S sand has spectacular lateral continuity, permitting consistent flow properties across the basin. The continuity and thickness of the sand is a product of the rapid subsidence in the Pliocene that constantly produced more accommodation space in this location (McGee, et al. 1994). The S is divided into 2 sand bodies separated by a 15 ft thick mudstone which is consistent across the basin, this horizontal impermeable layer prevents vertical flow (McGee, et al., 1994), but the good lateral fluid flow conditions remain unchanged.

### **The 'GREEN' sand**

The upper Pliocene Green sand exhibits a transition from lower sheeted sands to upper channelized sands, the sand is present across the

eastern half of the basin, but in the west and north it exhibits shingles, which may act as barriers to fluid flow (McGee, et al. 1994)

### **The 'BLUE' sand**

The mid Pleistocene Blue sand was deposited in a more channelized environment (McGee, et al., 1994). The main difference from the lower Green and Pink sands is that it has lower lateral continuity. Pinching and swelling of the seismic event imaging the sand were interpreted as north-south trending shingle boundaries (McGee, et al., 1994); these features may reduce the connectivity across the basin.

### **The 'YELLOW' sand**

The Yellow sand was deposited by channel systems with levees and shingles. As in the case of the Blue sand, these shingles may act as flow within the Yellow sand.

## **PRESSURE AND STRESS**

In passive margins, the lithostatic overburden stress ( $\sigma_v$ ) (see Table 2 for full nomenclature) is equal to the maximum principle stress and the minimum horizontal stress ( $\sigma_h$ ) is equal to the least principle stress (Turcotte and Schubert, 2002).  $\sigma_v$  at depth 'z' can be approximated by equation 1;

$$\sigma_v = 0.9(z - z_1) + (\rho_w g z_1) \quad (1)$$

Where  $z_1$ =seafloor depth in feet. So  $z-z_1$  (sediment thickness) is multiplied by the overburden stress gradient of 0.9psi/ft,  $(\rho_w g z)$  represents the hydrostatic pressure ( $P_w$ ) at the seafloor depth ( $z_1$ ) (equation 2), as at this point at the top of the sediment column,  $\sigma_v$  is equal to  $P_w$ .

$$P_w = \rho_w g z \quad (2)$$

Where  $\rho_w$ =water density (ppg),  $g$ =gravitational acceleration, and  $z$ =true vertical depth sub sea-surface (TVDSS) (ft).

The offset of the formation  $P_w$  (water pressure at the OWC) from the hydrostatic pressure ( $P_h$ ) is the water phase overpressure ( $P_w^*$ ):

$$P_w^* = P_w - P_h \quad (3)$$

### **Formation Pressures**

Pressures within the basin sands can be calculated by making extrapolations of pressure values from the formation fluid pressure ( $P_o$  (oil) or  $P_g$  (gas)) measured at the Auger field section in the east (Figure 1) down to the OWC at which point the pressure of the hydrocarbons (recorded) is interpreted as being equal to the pressure of the underlying water. Here the fluid pressure is extrapolated along the hydrostatic gradient, down to the synclinal low and then to the sand crest in the west (Figure 12) following the hydrostatic gradient at all times.

This simple extrapolation is based upon several significant assumptions. First we assume that the aquifer itself has sufficient permeability such that at any reasonable basin flow rates, the vertical pressure gradient always approximately follows the hydrostatic gradient and the overpressure is constant. Second, it is assumed that the pore throats in the reservoir are sufficiently large that the oil and water pressures are equal at the oil water contact.

Core data from the reservoir section of the Pink sand yield moderate permeabilities of 185-346mD in the upper sand body (Bilinski, et al., 1995).

The pre-production formation pressures of the Yellow, Blue, Green and Pink sands were estimated for all points within the basin using the method outlined above (Table 1). Overpressure in the different sand units varies from 3410 psi (Blue) to 4230 psi (Pink) but all overpressures were interpreted as being constant with depth. With these fluid overpressures and an overburden stress gradient of 0.9 psi/ft (Figure 11), it is predicted that the crests of all 4 sands are sufficiently overpressured to permit seal fracture and expulsion. For all 4 sands to be in the state of expulsion at their crests, permeability and hydraulic connectivity must remain high throughout the extent of the sand. McGee et al. (1994) remarked, however, that the lateral connectivity was greatest in the Pink sheet sand, and that the overlying sands possess either flow inhibiting properties or laterally discontinuities. Thus I interpret that the Pink sand the only sand with hydraulic connectivity between the reservoir section in the east and the sand crest in the west (Figure 5).

## Basin Leak Point

The point at which a sand pore pressure intersects the overburden stress is the basin leak point.

All sands are shallowest in the west of the basin where they onlap the western basin bounding ridge below GB Block 424 (Figure 1, 5, 10). At the western edge, the sand crests reach their shallowest depths (Table 1), and the several sand pore pressures converge on the overburden stress defined in Equation 1.

Depths to the sand crests were calculated from TWT (seismic Two Way Time) using sediment velocities calculated at the Auger field to the east where accurate depths to the horizons were interpreted from the well logs. Figure 3 plots the velocities calculated for several sand horizons of known depth (ft and TWT) with a line of best fit plotted to interpret the velocities at any depth. There is some degree of error in this inference as the greater water depth at the Auger field, and its effect on the compaction of the sediment has the effect of increasing seismic velocities. The velocities for the horizons were calculated using equation 3;

$$V_{\text{sediment}} = (z_2 - z_1) / (t_2 - t_1) \quad (3)$$

Where z=depth to the horizon in ft, t=one way time to the horizon in seconds, and 1=seafloor horizon depth and 2=sand horizon depth. See Table 1 for sand crest depths.

This depth minima of the Pink sand continues along strike continuously around the western limit of the Auger Basin, and continues north into the adjacent Andros Basin, and underlies several other expulsion features identified in previous studies (Aharon, 2003, MacDonald, et al. 1994, 2000) and other similar features identified but not further discussed in this study. The state of expulsion of these features is not only constrained by sand crest depth, but also by the thickness of overlying sediment. Expulsion only occurs at points of low overburden stress, and therefore areas of low sediment thickness (represented by bathymetric lows) are prone to expulsion.

## **SEAFLOOR EXPULSION FEATURES**

This study uses 3D multi-channel seismic software and the 2002 seismic survey data to locate seafloor expulsion features for further surface and subsurface interpretation.

The GB Block 424 feature labeled in Figure 1 is characterized in seismic section by a sub-vertical column of chaotic and low amplitude reflections (gas wipeout zone (GWZ)) (Figure 4). This column reaches the sediment surface at a depth of 560 m (1837 ft) below sea level. Here, there is a pronounced symmetrical bathymetric mound with a central depression exhibiting low amplitude reflectors (Figure 5). The bathymetric surface expression of the GB Block 424 feature shows an elliptical mound 666 x 833 m (2185 x 2732 ft) across with a central, flat-based depression, about 10 m lower than the surrounding rim, (see Figure 6). The perimeter rim of the Block 424 is broken at the northern margin by a 75 m wide channel. Figure 5

identifies low amplitude reflections within the central depression of the mound with higher amplitudes in the rim and adjacent seafloor. The low anomaly continues through the northern rim break increasing in amplitude down-dip on the northern slope of the mound. This low amplitude fan reaches 300m down-dip towards the basin floor.

Kieckhefer, et al., (2003) interpreted these anomalies as poorly consolidated sediment flows of ejected material from the seafloor expulsion features depositing down dip in fan like morphologies.

Further down the slope of the basin floor to the west, the low amplitude signature of these anomalies diminishes, and after around 300 m 'ambient' amplitude reflectors of the basin floor sediments (colored purple to dark blue in Figure 6) can be seen. Past this 300 m distance from the expulsion feature, only subtle variations in amplitude can be observed to suggest the presence of sediment fans, but in seismic section of the subsurface, distinct structures can be observed radiating out into the basin. The seismic sections of Figures 8 and 9 are spaced at 2 km, Figure 8 being 2 km from the centre of the GB Block 424 feature highlight a series of stacked erosional channels over a width of 3.5 km, Figure 9, 2km further down dip illustrates a similar 3.5 km-wide zone of channelization with a lower overall vertical thickness. These units can be traced as far as the centre of the basin, approximately 6km from the source.

The vent of Block 424 was surveyed by acoustic echo soundings from a near sea-bed submersible by Sager et al. (1999). Further direct imaging and analysis of the subsurface through piston cores were used to provide ground truths for the interpretation of acoustic sounding zones. Sager et al.

(1999) identified a number of active gas/fluid vents within the central depression of the GB Block 424 feature. In areas around these vents, piston cores penetrated authigenic carbonates and gas hydrates, while visual observations identified live communities of chemosynthetic organisms living on and around the vents. Analysis of the same feature by in 1997 and 1998 (MacDonald, et al., 2000) identified high molecular weight hydrocarbons in the immediate subsurface of the venting areas, but only low levels of expulsion of these denser oils in the area during the 2 submersible missions.

## **Discussion**

The GB Block 424 seafloor expulsion feature contains authigenic carbonates, chemosynthetic communities, gas hydrates and high molecular weight hydrocarbons (Sager, et al., 1999, MacDonald, et al., 2000). The expulsion feature itself also displays low amplitude anomalies in the central surface area (Figure 6), a distinct GWZ (Figure 4) and active gas vents within the central dome (Sager, et al. 1999). These are features associated with active expulsion (Seldon and Flemings, 2005, Macdonald, et al., 1990).

Seismic data record a gas wipeout zone (GWZ) that is interpreted to be sediment with fluid and gas-filled pore spaces. This wipeout zone extends several hundred feet below to the seafloor feature (Figure 4).

What distinguishes the feature of GB Block 424 from previously studied expulsion features (Seldon and Flemings, 2005, Aharon, 2003, MacDonald, et al. 1994, Sager, et al., 1999) is that there is a poorly developed record of sediment extrusion. Furthermore, these deposits have

low amplitude reflections that emanate from the central dome on the seafloor (Figure 5). The low amplitude signature fan can only be clearly identified to a distance of 300m into the basin down dip of the vent. This is much more limited than the 6-8 km long fans interpreted in other Gulf of Mexico expulsion settings (Aharon, et al., 2003, Seldon and Flemings, 2005). We interpret that the low amplitude deposits to be vent-derived. The small extent of these deposits suggests minor expulsion in recent times.

The Pink sand pore pressure converges on, but does not exceed the overburden stress (Figure 11). This is because the overburden stress acts as a limit, and at any time when the pore pressure exceeded this limit, fluid expulsion would occur, venting pore pressure until the pressure falls back below the confining overburden stress, and re-equilibrating the pore pressure with the overburden stress. At this point fluid expulsion from the leak point will cease, and the pressure field is once again in equilibrium.

The basin leak point is located in this study below the GB Block 424 feature as this is the point of minimum depth of the Pink sand, from which the fluid is sourced. An expulsion feature occurs at this point because the sediment thickness above the over-pressured Pink sand crest is lower than at other points along the crest line, the sand crest is shallower, and therefore the net overburden stress is lower.

Extrapolation of pressure from the data points of the Auger field infers that all four sand bodies have pore pressures that converge on the overburden stress at the sand crest basin leak point (Figure 11). This extrapolation process is outlined in Figure 12. We propose that although all 4 predicted sand pressures converge on the local overburden stress at their

crests, only the Pink sand is actively involved in fluid expulsion. The lack of hydraulic connectivity between the reservoir section and the sand crests in the Green, Blue and Yellow sands will have the effect of inducing compartmentalization of the sand pressure zones, reducing the maximum pore pressure at the sand crest. Furthermore chemical analysis of the fluids of the GB Block 424 feature by MacDonald, et al. 2000 indicated the presence of high molecular weight hydrocarbons, characteristic of the lower sands of the Auger field (Bilinski, et al. 1995)).

The interpreted pulsed nature of expulsion from the GB Block 424 feature may be attributed to a number of parameters. As expulsion only occurs when the pore pressure ( $P_w$ ) exceeds the overburden stress ( $\sigma_v$ ), if  $P_w$  periodically falls, or  $\sigma_v$  episodically rises, expulsion will cease. Rise in sea level, or increased sedimentation rates to the seafloor locally will both increase overburden stress. Conversely, falling reservoir pressure associated with production from the Auger field in the east will potentially impede expulsion. These processes may be similarly effective on defining the 'on/off' state of the expulsion features of the basin.

We propose that the lack of low amplitude fans at the sediment surface down dip of the GB Block 424 feature is a response to the pulsed nature of sediment ejection from the vent, and the intermittent deposition of down-dip fans of sediment interspaced with the deposition of hemipelagic silts and clays. This interpretation suggests that the 2002 seismic survey captured the GB Block 424 feature during a period of inactivity, following a period of previous activity recorded by chaotic erosive seismic facies in the subsurface.

Since these 'expulsion events', the feature has become inactive and ambient hemipelagic deposition has returned to the surrounding basin floor.

## **Conclusions**

A number of conical, elliptical/circular mounds on the eastern rise of the western basin bounding ridge of the Auger basin, deep water Gulf of Mexico (Figure 1), can be interpreted as sea-floor fluid/mud expulsion features. The key characteristics of active mud volcanoes as recorded in seismic data are; Sub-vertical chaotic columns with reflection wipeout below the sea-floor mound (similar features in the Popeye field were interpreted as 'gas wipe-out zones' by Brookes, et al., (1986)), Conical/domed symmetrical mounds which enclose a flat based, central depression with hydrocarbon saturated sediment cover and expulsion vents and sediment fans emanating from the central mound.

The pressure within the Pink sand of the Auger basin is limited to that of the overburden at the basin leak point, and the basin leak point is located where the reservoir is at its shallowest, and where subsequent sediment cover is at its thinnest. The Pink sand, a major hydrocarbon pay of the Auger field has undergone cyclic expulsion from the basin leak point below GB Block 424 during times when its fluid pressure exceeds the overburden stress. These events are recorded by fans of sediment deposited down dip into the basin center. This expulsion and deposition of sediment is a cyclic process, and a number of parameters including sea level change, sedimentation rate and hydrocarbon production from the Auger field currently

reduce the pore pressures below the overburden stress sufficiently so that the expulsion feature is inactive.

The understanding of the limit to reservoir pressure (local overburden stress) at the sand crest has implications effecting the production at the hydraulically connected Auger field. Recognition of reservoir pressure may be used to mitigate problems such as oil slick generation and slope oversteepening and failure (related to ejected material buildup) associated with seafloor expulsion, making it possible to design safer rig moorings and ease the environmental impact of hydrocarbon extraction.

## **ACKNOWLEDGEMENTS**

This work would not have been possible without the guidance and support of my advisor Dr Peter B. Flemings. His assistance gave me direction and inspiration throughout. Furthermore I thank Heather Nelson for her patience in assistance countless software queries, and Matthew Reilly and Charles Bohn of the Geosystems Initiative (Team 4) for their discussions and advice. Finally I thank Dr Dave Bice, as through his input; I have gained much over the past year.

## **References**

- Aharon, P., 2003, Is Drilling in Deepwater Gulf of Mexico Uncorking Bad Genies? GCAGS 53rd Annual Convention, Baton Rouge, Louisiana.
- Anderson AL and Bryant WR (1990) Gassy sediment occurrence and properties: northern Gulf of Mexico. *Geo-Marine Letters*

10 : 209-220.

- Bilinski, P.W., McGee, D.T., Pfeiffer, D.S., Shew, R.D., 1995, Reservoir Characterization of the "S" Sand Auger Field, Garden Banks 426, 427, 470, and 471, Shell Offshore Inc., New Orleans, Louisiana, and Shell Oil Company, Houston Texas, p. 75-93.
- Bohn, C., 2006, Bathymetric basemap of the Gulf of Mexico with Auger highlighted.
- Booth, J.R., Dean, M.C., DuVernay, A.E., Styzen, M.J., 2003, Paleobathymetric controls on the stratigraphic architecture and reservoir development of confined fans in the Auger Basin: central Gulf of Mexico slope, *Marine and Petroleum Geology*, v. 20, p. 563-586.
- Brooks, J. M., H. B. Cox, W. R. Bryant, M. C. Kennicutt, II, R. G. Mann, and T. J. McDonald, 1986, Association of gas hydrates and oil seepage in the Gulf of Mexico, *in* D. Leythaeuser and J. Ruellkotter, eds., *Advances in organic geochemistry: Organic Geochemistry*, v. 10, p. 221–234.
- Cathles, L. M., and A. T. Smith, 1983, Thermal constraints on the formation of Mississippi Valley-type lead-zinc deposits and their implications for episodic basin dewatering and deposit genesis: *Economic Geology*, v. 78, p. 983– 1002.
- Flemings, P. B., Stump, B. B., Finkbeiner, T. and Zoback, M. 2002, Flow focusing in overpressured sandstones: Theory, observations, and applications: *American Journal of Science*, v. 302, p. 827– 855.
- Harrison, W. J., and L. L. Summa, 1991, Paleohydrology of the Gulf of Mexico basin: *American Journal of Science*, v. 291,

p. 109– 176.

Hubbert, M. K., and D. G. Willis, 1972, Mechanics of hydraulic

fracturing: AAPG Memoir 18, p. 239– 257.

Kieckhefer, R.M.; Herkenhoff, E.F.; Wright, J.Q.; Mollenkopf, R.; Smith, N.;

Kuliyeva, R.; Connor, J.A. 2003, Sea-floor properties from the

inversion of 3D multichannel seismic data: a submarine mud-volcanic

flow in the Absheron block, offshore Azerbaijan OCEANS 2003.

Proceedings, Vol.5, Iss., 22-26 Sept. 2003 Pages: P2727- P2734 Vol.5

Lee, C.S., (1995) Geology of hydrocarbon seeps on the northern Gulf

of Mexico continental slope. Unpublished PhD thesis. College

Station: Texas A&M University, 114 pp

MacDonald IR, Guinasso NL, Reilly JF, Brooks JM, Callender

WR, and Gabrielle SG (1990) Gulf of Mexico hydrocarbon seep

communities: VI. Patterns of community structure and habitat.

Geo-Marine Letters 10 : 244-252

MacDonald, I. R., Guinasso, N. L., Sassen, R., Brooks, J. M., Lee, L., and

Scott, K. T., 1994, Gas hydrate that breaches the sea floor on the

continental slope of the Gulf of Mexico: *Geology*, v. 22, p. 699-702.

MacDonald, I.R., Buthman, D.B., Sager, W.W., Peccini, M.B., Guinasso, N.L.,

Jr., 2000, Pulsed Oil Discharge from a Mud Volcano, *GSA Bulletin*, V.

28, No. 10, p. 907-910.

McGee, D. T., Bilinski, P. W., Gary, P. S., Pfeiffer, D. S., and Sheiman, J. L.,

1994. Geologic Models and geometries of Auger field, deep-water Gulf

of Mexico, *in* Weimer, P., Bouma, A. H., and Perkins, B. F., eds.,

*Submarine Fans and Turbidite Systems—Sequence Stratigraphy*,

Reservoir Architecture, and Production Characteristics:GCSSEPM,  
15<sup>th</sup> Annual Research Conference, p. 245-256.

Mutti, E. and Normark, W.R. (1987). Comparing examples of modern and ancient turbidite systems: Problems and concepts. In: J.K. Legget and G.G. Zuffa (eds.). Deep Water Clastic Deposits: Models and Case Histories. Graham and Trotman, London, p.1-38.

Mutti, E. and Ricci Lucchi, F. (1972). Le torbiditi del l'Apennino sttentrionale: introduzione all'analisi di facies. Memoir Societa Geologica Italiana, Vol. 11,, p.161-199.

National Geophysical Data Center, 1998,

<http://www.ngdc.noaa.gov/mgg/bathymetry/hydro.html>

Normark, W.R. 1978. Fan valleys, channels, and depositional lobes on modern submarine fans : Characters for recognition of sandy turbidite environments. American Association of Petroleum Geologists Bulletin, Vol.62, p.912-931.

Prather, B.E., 2000, Calibration and Visualization of Depositional Process Models for Above-Grade Slopes: a Case Study from the Gulf of Mexico, Marine and Petroleum Geology, V. 17, p. 619-638.

Prather, B.E., Booth, J.R., Steffens, G.S., Craig, P.A., 1998, Classification, Lithologic Calibration, and Stratigraphic Succession of Seismic Facies of Intraslope Basins, Deep-Water Gulf of Mexico, AAPG Bulletin, V. 82, No. 5A, p. 701-728.

Roberts HH, Aharon P, Carney R, Larkin J, and Sassen R (1990) Sea floor response to hydrocarbon seeps, Louisiana continental slope. Geo-Marine Letters 10 : 232-243

Sager, W.W., Lee, C.S., Macdonald, I.R., and Schroeder, W.W., 1999, High-frequency near-bottom acoustic reflection signatures of hydrocarbon seeps on the northern Gulf of Mexico continental slope: *Geo-Marine Letters*, v. 18, p. 267–276.

Seldon, B.J., Flemmings, P.B., 2005, Reservoir pressure and seafloor venting; predicting trap integrity in a Gulf of Mexico deepwater turbidite minibasin, *AAPG Bulletin* (January 2005), 89(2):193-209

Turcotte, D. L., and G. Schubert, 2002, *Geodynamics*: Cambridge, Cambridge University Press, 456 p.

Walker, R.G. (1978). Deep-water sandstone facies and ancient submarine fans: models for exploration for stratigraphic traps. *American Association of Petroleum Geologists Bulletin*, Vol. 62, No.6, pp.932-966.

	Reservoir Repeat Formation Test				Hydrocarbon-Water Contact (OWC)		
Sand	Fluid Pressure (psi)	Fluid Type	TVDSS (ft)	Sand Crest TVDSS (ft)	Fluid Pressure (psi)	Hydrocarbon – water contact depth (ft)	Pw* (psi)
Yellow	10465.2	Gas	15266	7961.047	10552.4	15498	3756.6
Blue	10507.0	Gas	15954	8366.425	10593.2	16203	3410.4
Green	12005.50	Oil	17420	10060.36	12094.9	17675	4261.8
Pink	12782.0	Oil	18972	11443.85	12941.0	19650	4230.2

**Table 1: Pre-production Formation Pressures of the Auger sands. Arbitrary single repeat formation test values are given for each sand including fluid pressure, fluid type and depth. Sand crest depth was interpreted from multichannel seismic data, and HWC pressures and depths were calculated from extrapolating the appropriate fluid**

pressure gradient to the depth of the HWC.  $P_w^*$  is simply the local pore pressure minus the local hydrostatic pressure.

**Table 2: Nomenclature**

<b>Variable</b>	<b>Description</b>	<b>Units</b>
$g$	Gravitational acceleration	$\text{ft s}^{-2}$
$P_h$	Hydrostatic pressure	Psi
$P_o$	Oil pressure	Psi
$P_g$	Gas pressure	Psi
$P_w$	Water pressure	Psi
$P_w^*$	Water overpressure	Psi
TVDSS	True vertical depth beneath sea surface	Ft
$\sigma_v$	Overburden stress	Psi
$\rho_w$	Water density	Ppg

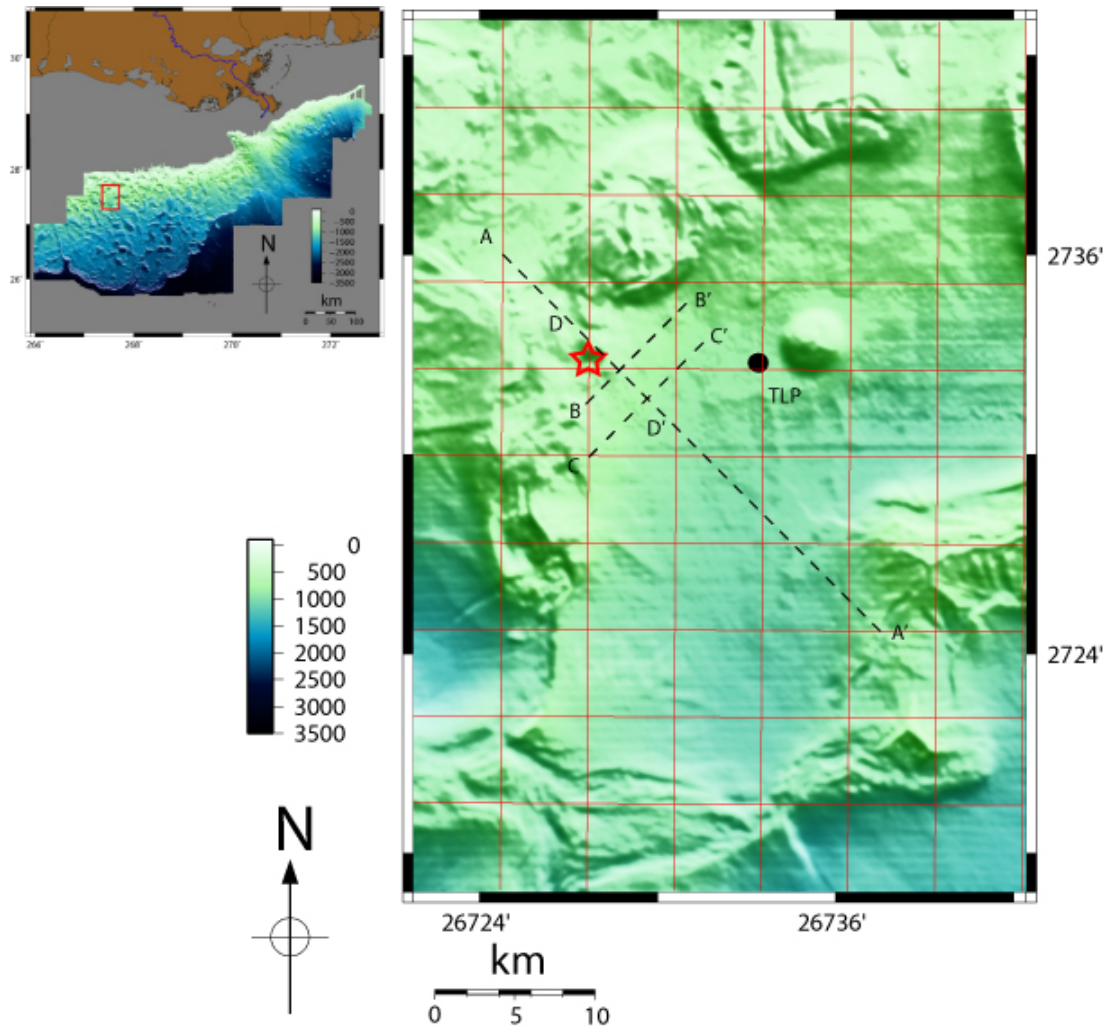


**Figure 1: Bathymetric Contour map of the Auger Basin with inset map (modified from Bohn, C., 2006) indicating position of the Auger Basin 220 miles south west of New Orleans, Louisiana. Highlighted is the Auger Tension Leg Platform (TLP), and the area covered by detailed bathymetric and amplitude extraction maps (red square) and the GB Block 424 expulsion feature (star).**

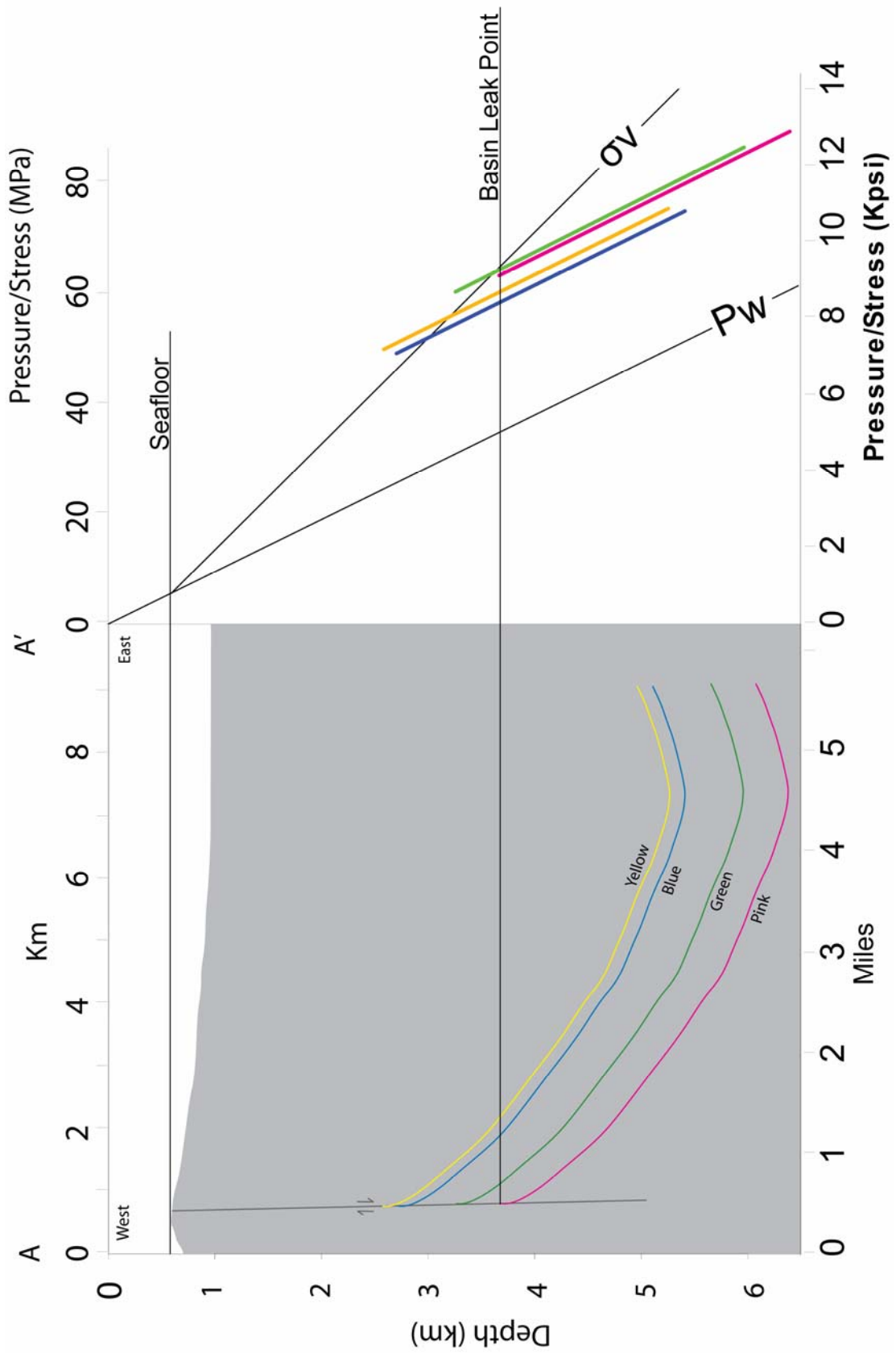
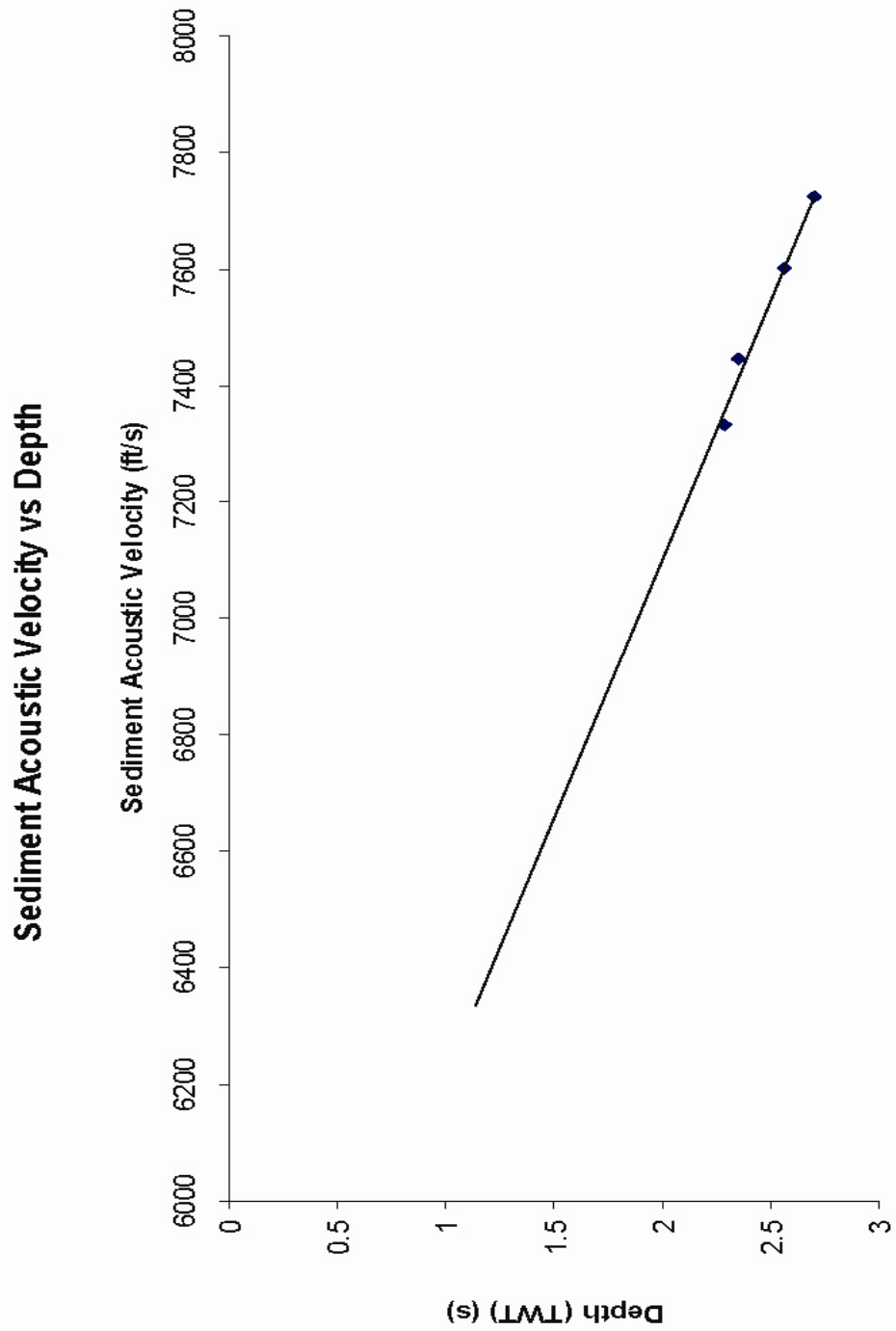
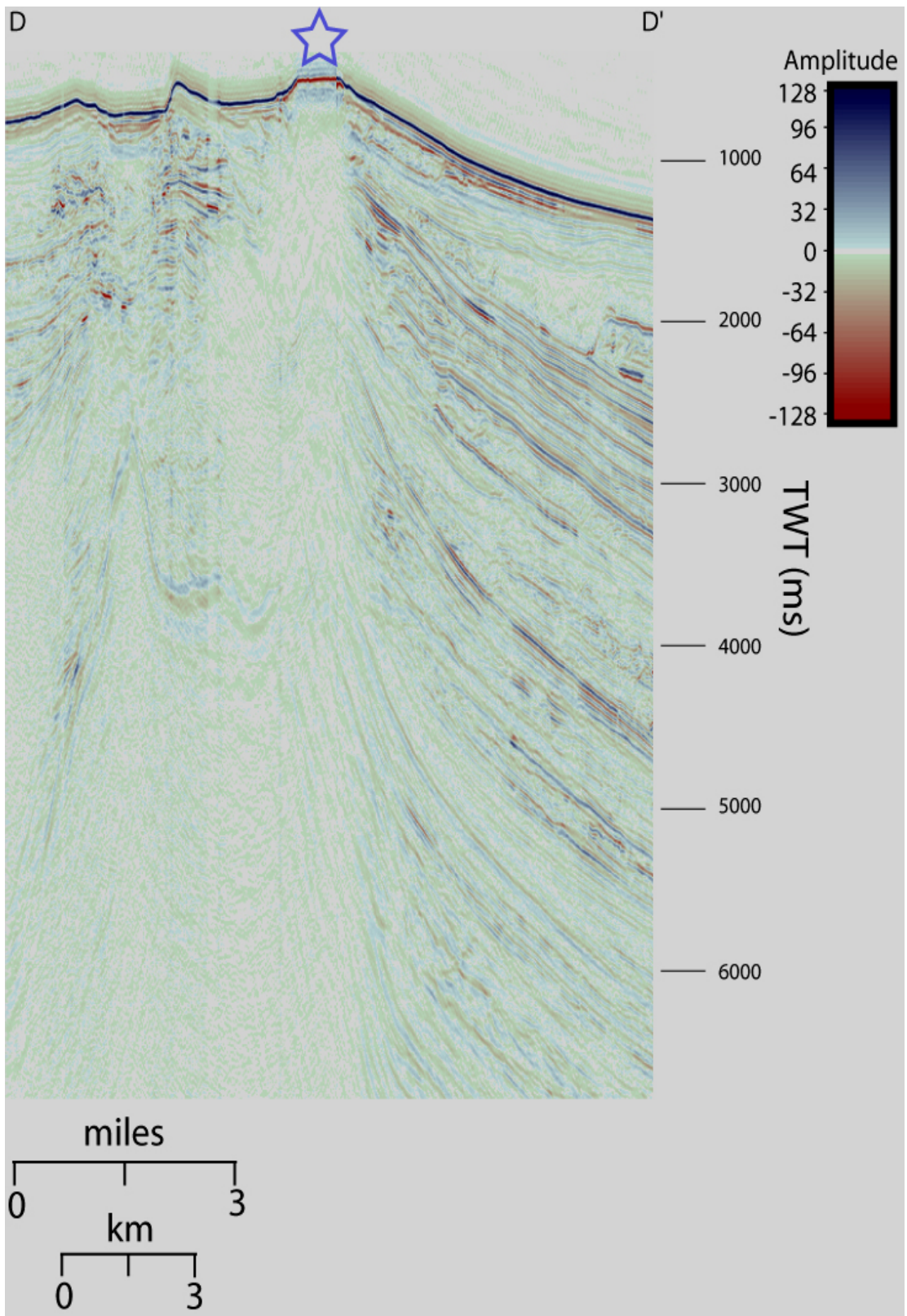


Figure 2: Schematic geological line of section and associated pressure fields in the Auger Basin. The Pink sand is interpreted to be at the state of expulsion.



**Figure 3: Sediment velocity vs. depth. Values calculated from the TWT and known depths of 4 sand horizons of the Auger field. The line of best fit is used to infer velocities for areas of known TWT.**



**Figure 4: Seismic signature of the GB Block 424 expulsion feature (below star) highlighting the reflector wipe-out beneath the feature. (Line of section marked on figure 1).**

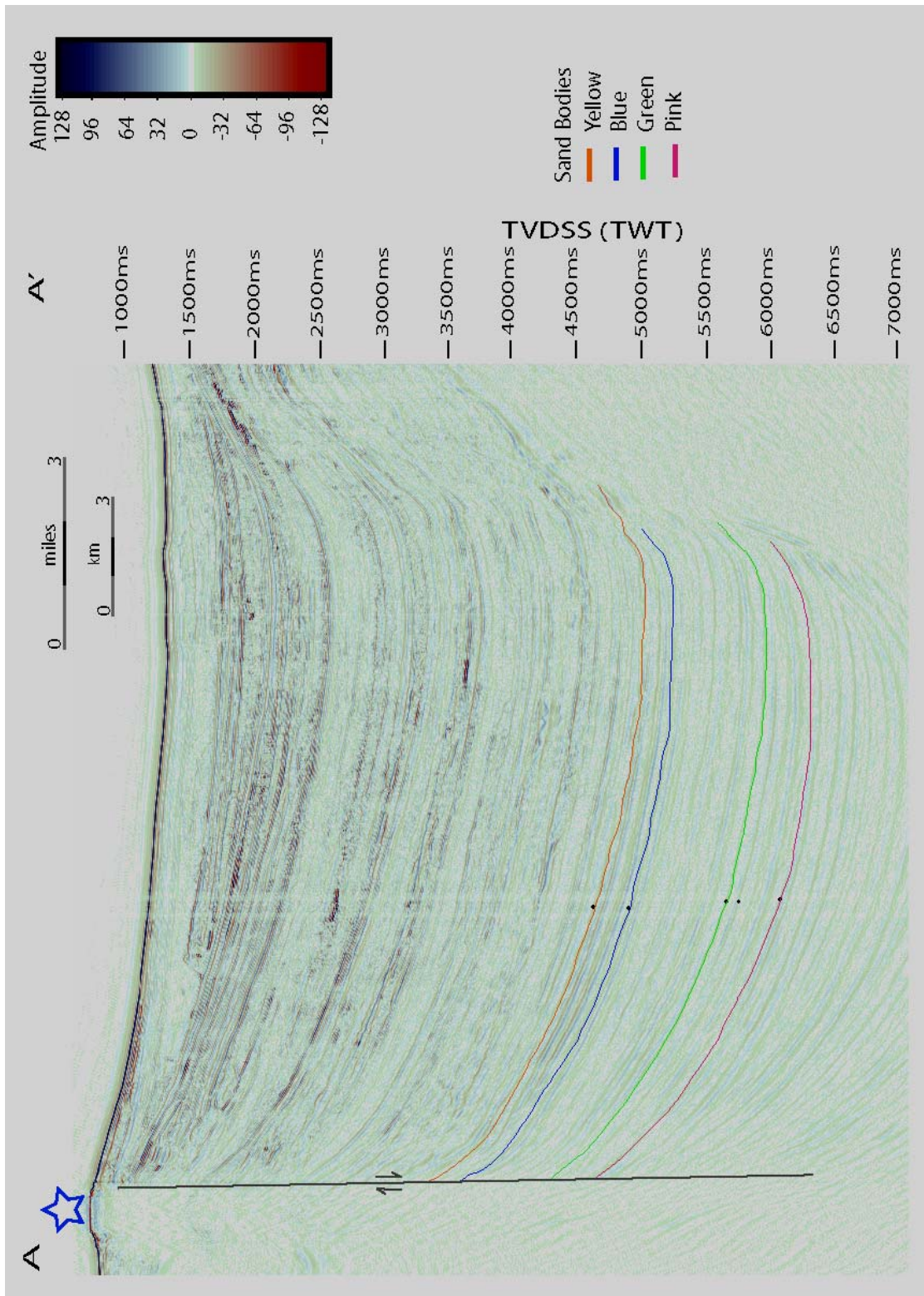
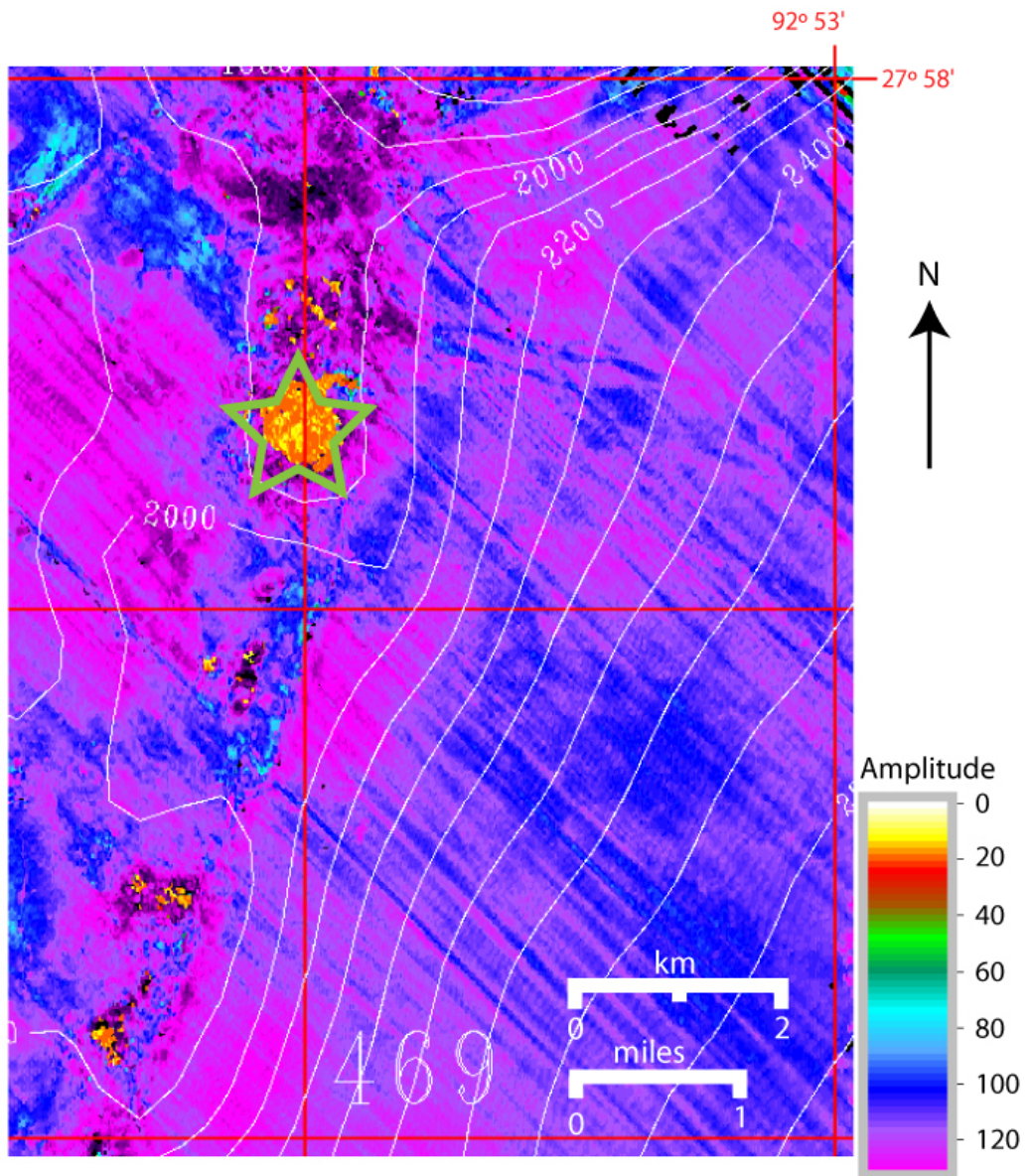


Figure 5: Seismic section of the GB Block 424 feature along line of section plotted on figure 1. Salt related fault in the north west has movement sense annotated (note fault dip is exaggerated by vertical exaggeration. Reservoir sands of the Auger Field are illustrated and the expulsion feature of block 424 is indicated (star).



**Figure 6: Amplitude extraction map of the region highlighted in figure 1 with bathymetric (feet below sea level) contours overlain. Encompassing the GB Block 424 expulsion feature surveyed (Star).**

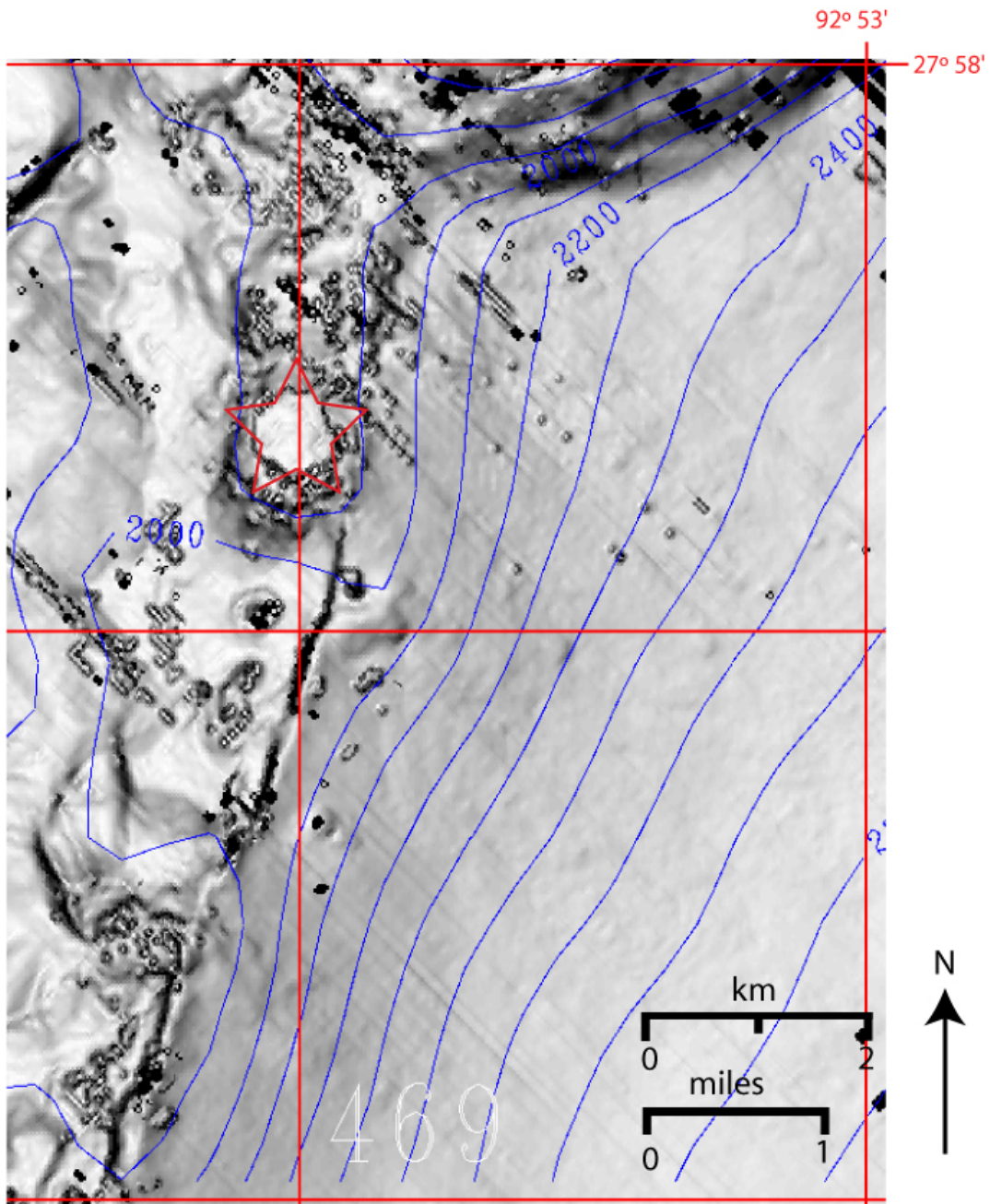


Figure 7: Seafloor bathymetric structure map of GB Blocks 425/426 (highlighted in Figure 1) encompassing the GB Block 424 expulsion feature (Star). Light colors indicate low gradient, and dark colors indicate more significant gradients, notice the steeply dipping sides of the labeled expulsion feature.

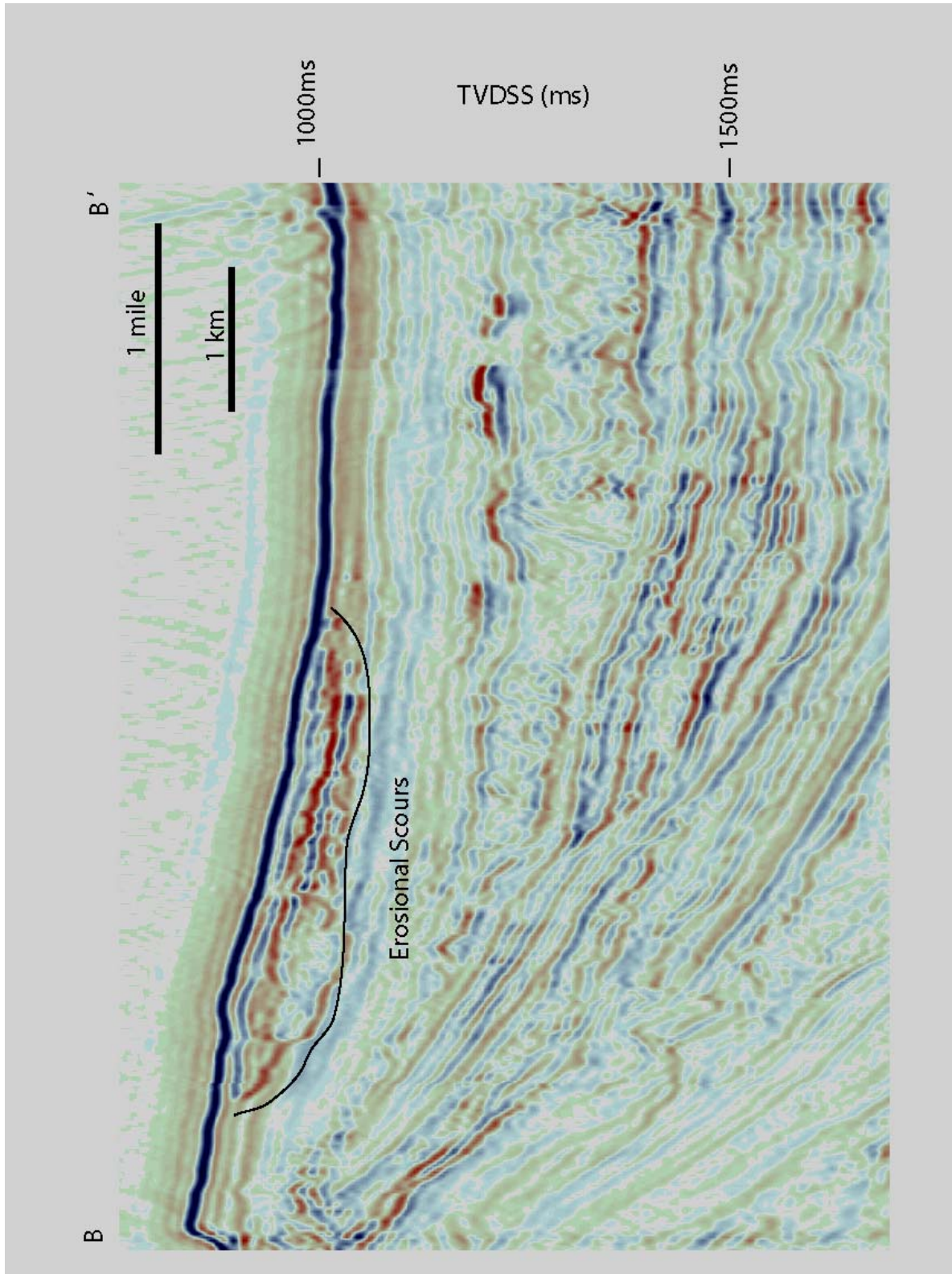
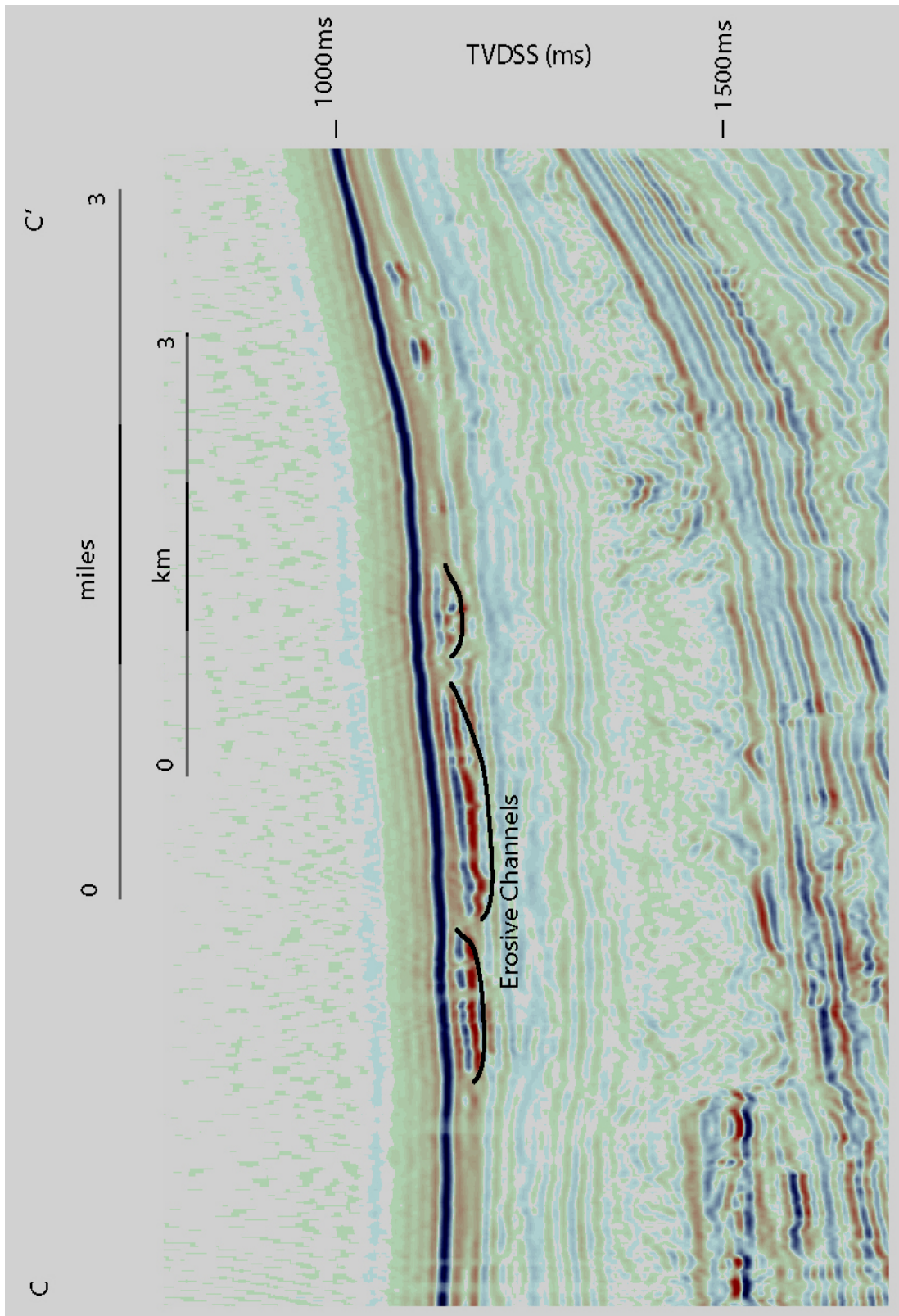
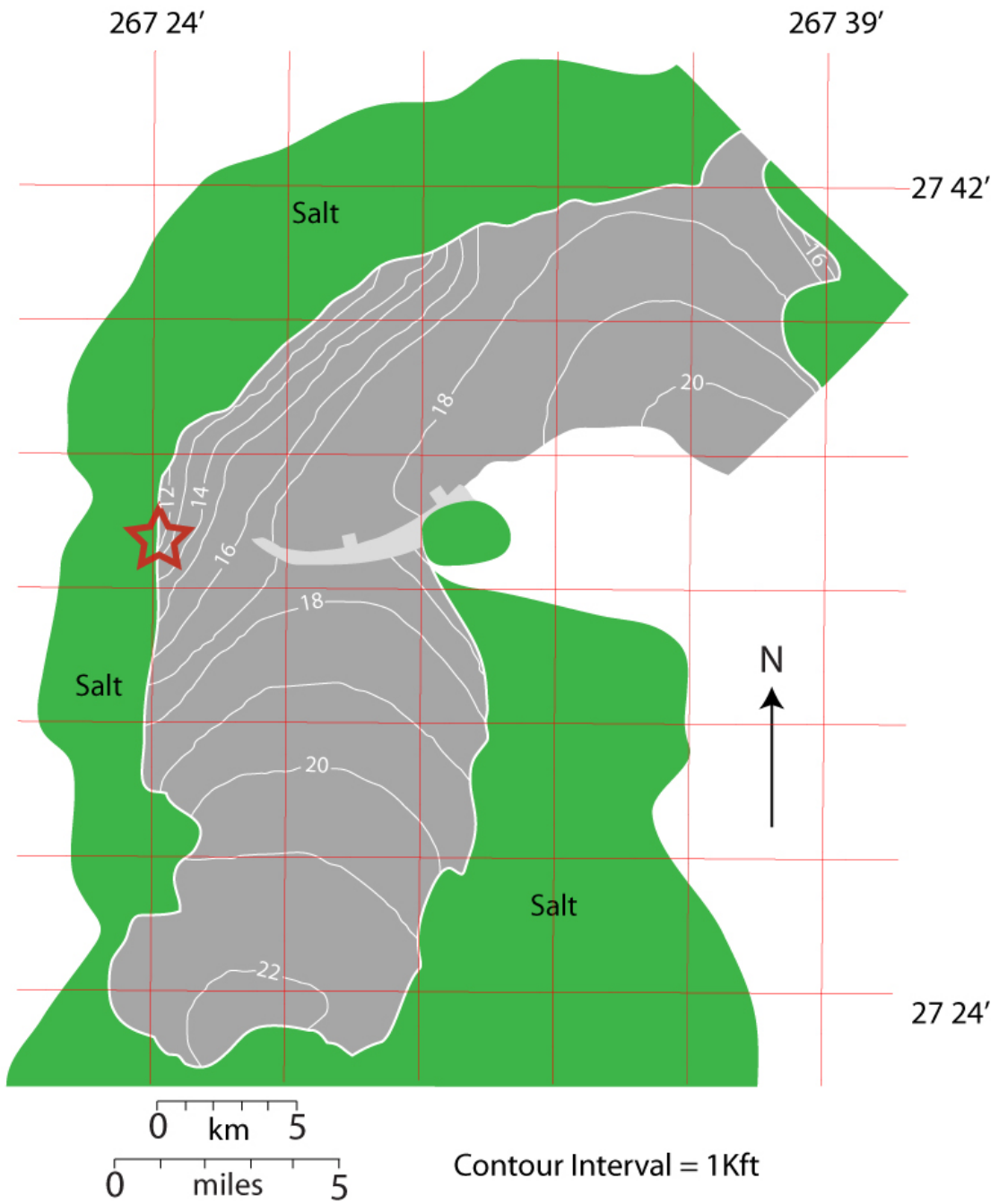


Figure 8: Section B – B' annotated in figure 1 highlighting the erosive channel incisions of flows sourced from the GB Block 424. The line of section is sub-perpendicular to seafloor dip at approximately 2km down dip from the expulsion feature of Block 424.



**Figure 9: Section C – C' annotated in figure 1 highlighting the erosive channel incisions of flows sourced from the GB Block 424 feature in a more distal setting. The line of section is sub-perpendicular to seafloor dip at approximately 4km down dip from the expulsion feature of Block 424.**



**Figure 10: Structure map of the Pink sand with 3x3 mile lease Block boundaries overlain. The boundaries were determined when the seismic signature of the unit became irregular, or at abrupt terminations in instances where the unit onlaps onto fault planes or salt. The figure highlights the down to the north 'North Auger Fault' (grey) which offsets the sand by several hundred feet.**

Pressure distribution below the GB Block 424 expulsion feature

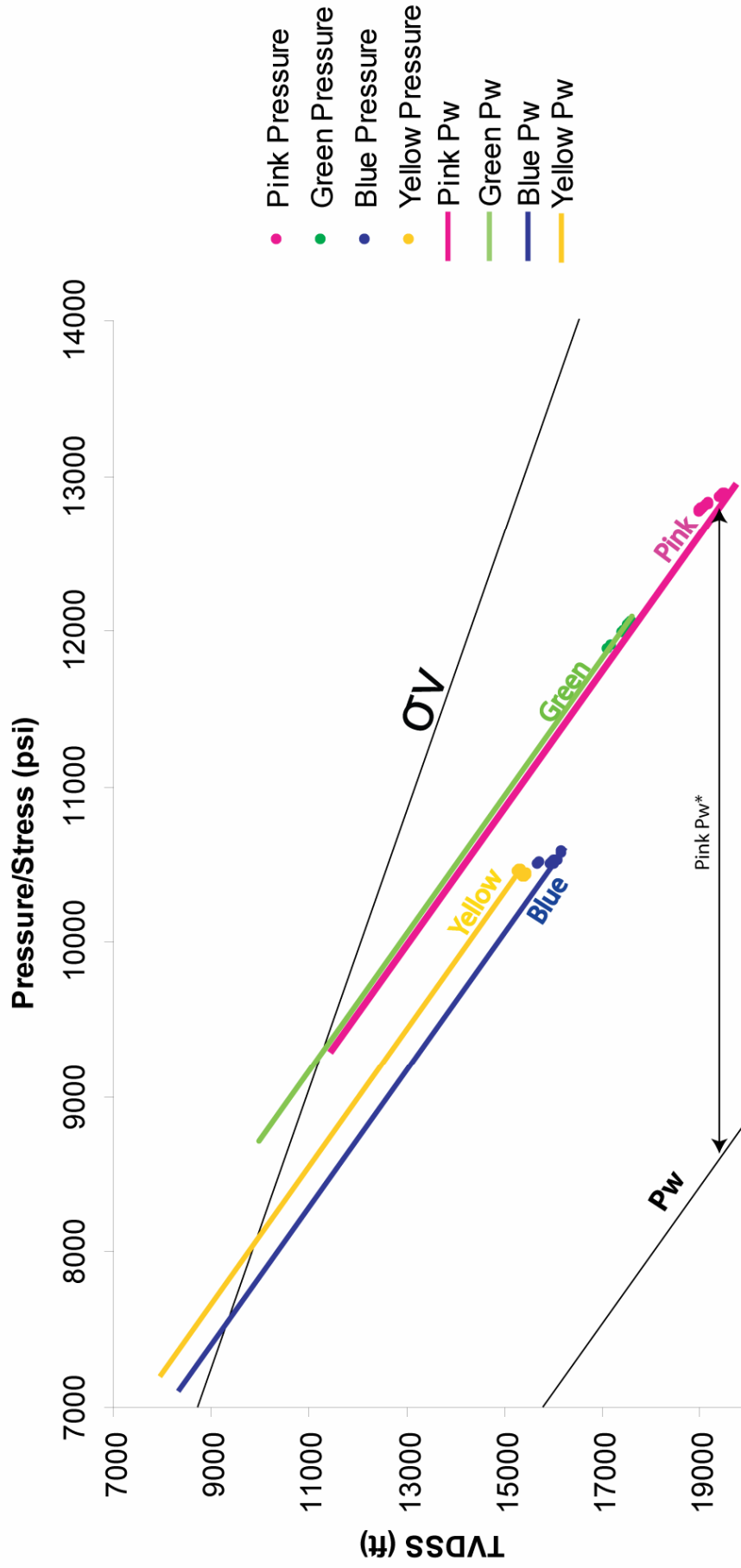


**Figure 11: Pressures and stresses below the GB Block 424 expulsion feature, hydrostatic pressure ( $P_w$ ), overburden stress ( $\sigma_v$ ) and the reservoir sand pressures ( $P_w$ ) of the Pink, Green, Blue and Yellow sands are shown. The plotted points for each sand aquifer are the pre-production sand pressures measured in the reservoir section in the east of the basin (Figure 1) Fluid pressures below the hydrocarbon-water contact (HWC) are projected to the point of minimum depth at the sand crest, to plot the pore pressure at this point. Data relating to the depths of the HWC, sand crest .and pressure measurements are recorded in Table 1, as well as typical pressure values for the Auger field Sands. See Figure 12 and text for discussion of the method for this extrapolation.**

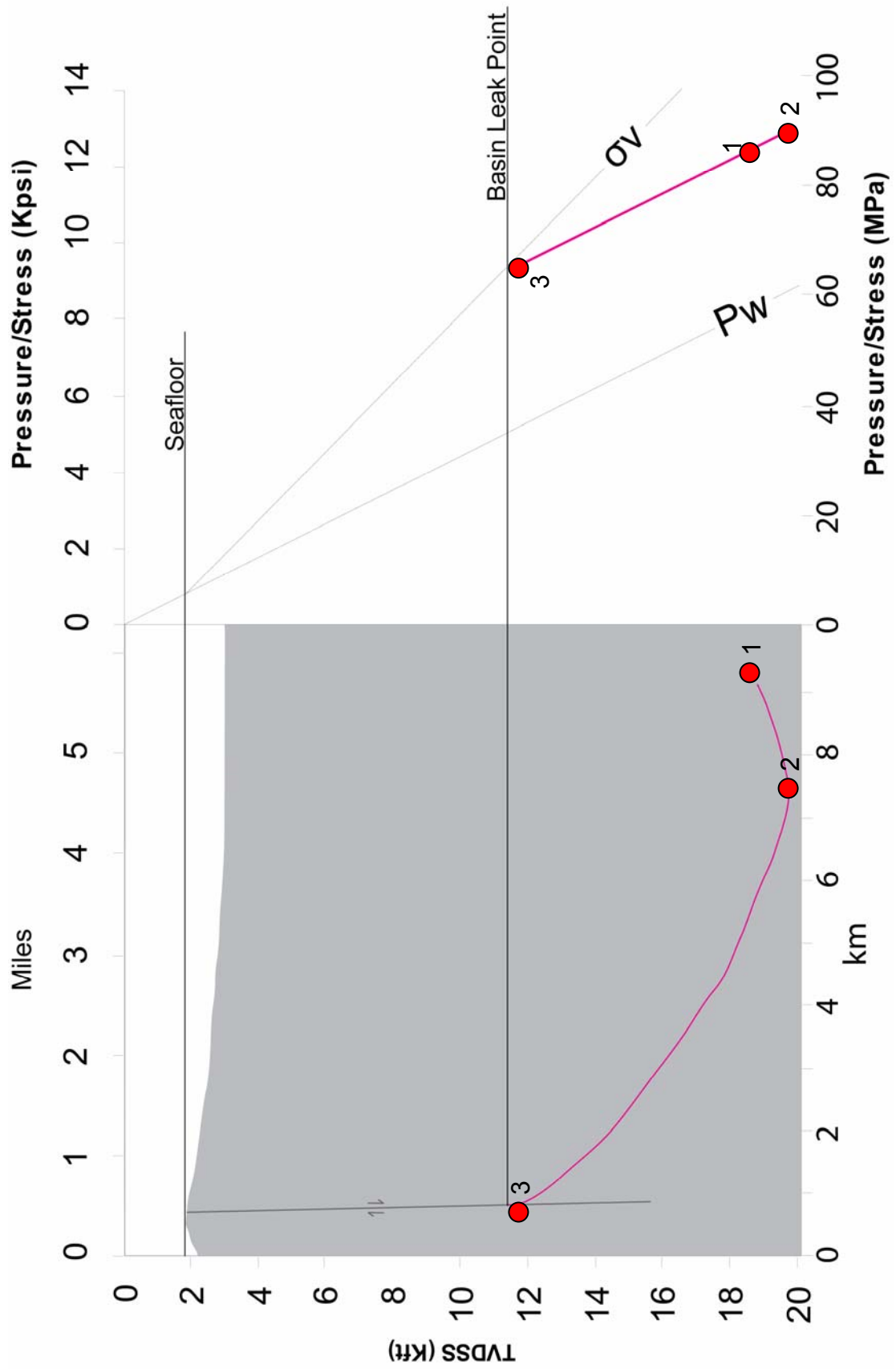


**Figure 12: Schematic geological line of section and associated pressure fields in the Pink sand of the Auger Basin. The pressure values of the reservoir section in the east (Point 1) were extrapolated along the hydrostatic gradient to the synclinal low (Point 2) and then to the sand crest in the west of the basin (Point 3).**